Fabrication of ZrC/SiC, ZrO_2/SiC and ZrO_2 powders by carbothermal reduction of $ZrSiO_4$

Ljiljana Kljajević[1], Branko Matović[1], Snežana Nenadović[1], Zvezdana Baščarević[2], Nikola Cvetićanin[3], Aleksandar Devečerski[1,*]

[1]*Department of Material Science, INN Vinča, University of Belgrade, Belgrade, Serbia*
[2]*Institute for Multidisciplinary Research, Materials Science Dept., Kneza Višeslava 1, University of Belgrade, Belgrade, Serbia*
[3]*Faculty of Physical Chemistry of Belgrade, University of Belgrade, Belgrade, Serbia*

Received 1 April 2011; received in revised form 21 May 2011; accepted 29 June 2011

Abstract

The zirconia/silicon carbide (ZrO_2/SiC) and ZrO_2 powders are prepared by carbothermal reduction of natural mineral zircon ($ZrSiO_4$). The zircon powder was mixed with activated carbon as a reducing agent and heat-treated in a controlled flow atmosphere of Ar. Phase evolution and phase content were followed as a function of temperature (1573–1973 K) and C/$ZrSiO_4$ ratio (C/$ZrSiO_4$ = 1, 4, 5 and 7), by means of ex-situ X-ray diffraction and SEM/EDS analysis. By varying the temperature and C/$ZrSiO_4$ ratio, different powder compositions were obtained (m-ZrO_2; m-ZrO_2/c-ZrO_2; c-ZrO_2; c-ZrO_2/SiC).

Keywords*: zirconia, silicon carbide, zirconium carbide, zircon*

I. Introduction

In recent years, there is a trend of developing technologies for producing refractory oxide-nonoxide composite materials [1–5]. By combining excellent properties of each component in composite material, the high temperature properties of the composite materials can be improved greatly. Zirconia and silicon carbide belong to the group of structural ceramics due to their excellent properties such as high fracture strengths, high temperature resistances, high erosion resistance as well as chemical resistance [6].

Zirconia (ZrO_2) is an important material in industry and technology because of its high melting point, low thermal conduction and high ionic conductivity. It is generally accepted that monoclinic form of ZrO_2 (m-ZrO_2) is stable below 1443 K, tetragonal form (t-ZrO_2) between 1443 K and 2643 K, and cubic form (c-ZrO_2) above 2643 K [7]. The high temperature cubic phase, which possesses better mechanical properties can be stabilized to room temperature by incorporating dopants in the crystal lattice (CaO, MgO, Y_2O_3, etc.).

* Corresponding author: tel: +381 11 3408 795
fax: +381 11 3408 224, e-mail: *drak@vinca.rs*

Pure $ZrSiO_4$ decomposes into ZrO_2 and amorphous SiO_2 at temperatures higher than 1723 K, as it was shown by the extensive *in-situ* study of $ZrSiO_4$ thermal decomposition performed by Kaiser *et al*. [8].

$$ZrSiO_4 = ZrO_2 + SiO_2 \quad (1)$$

This study also reveals isostructural transformation of t-$ZrSiO_4$→t-ZrO_2 in 1723–1973 K temperature region. However, if samples are allowed to cool spontaneously, m-ZrO_2 is obtained. It was also found that the presence of impurities (Al_2O_3, Fe_2O_3, TiO_2, etc.) reduces the temperature needed for $ZrSiO_4$ decomposition by formation of low temperature eutectic melts.

On the other hand, if ZrO_2 is obtained by ZrC oxidation, isostructural transformation c-ZrC→c-ZrO_2 takes place [9]. A considerable amount of carbon was detected in c-ZrO_2 phase, with highest concentration being measured at the ZrC/ZrO_2 interface. Considering literature data and their own results, Luo *et al*. [10] also suggested that carbon can help c-ZrO_2 stabilization in two ways: i) by surrounding c-ZrO_2 nanoparticles and preventing their aggregation and ii) by incorporating into the interstitial positions in ZrO_2. High surface tension is also responsible for appearance of

tetragonal phase at room temperature in undoped zirconia nanoparticles [11,12].

The process of carbothermal-reduction (CTR) implies reduction of oxygenated materials such as silica (SiO_2), for example, by mixing it with a reducing agent (carbon) at the temperatures usually higher than 1873 K, for several hours under an inert atmosphere. The formation of the final product is very complex and involves many intermediate stages [6,13,14]. The CTR method is economically attractive production route considering the fact that it uses naturally occurring materials and that the powders obtained in this way are usually perfectly homogenized.

By varying the $C/ZrSiO_4$ ratio, it is possible to obtain ZrO_2, ZrO_2/SiC or ZrC/SiC as zircon carbothermal reduction reaction products [4,5,11–13,15]:

$$ZrSiO_4 + C = ZrO_2 + SiO_{(g)} + CO_{(g)} \quad (2)$$

$$ZrSiO_4 + 3C = ZrO_2 + SiC + 2CO_{(g)} \quad (3)$$

$$ZrSiO_4 + 6C = ZrC + SiC + 4CO_{(g)} \quad (4)$$

Other experimental parameters like heating/cooling rate, static/dynamic atmosphere, presence of impurities, could also affect the reaction. For example, the form of obtained ZrO_2 (monoclinic, tetragonal or cubic) seems to be dependent on the cooling rate, the presence of excess carbon, the presence of additives and/or impurities, etc.

Formation of SiC from silica is usually represented by the following general reaction:

$$SiO_{2(s)} + 3C_{(s)} = SiC_{(s)} + 2CO_{(g)} \quad (5)$$

The formation of the final product is far more complex than the above equation shows, since (depending on experimental conditions) the process of SiC formation may consist of a series of solid-solid, solid-gas and gas-gas reactions [13,16,17].

Formation of ZrC from zirconia is usually represented by following general reaction:

$$ZrO_2 + 3C = ZrC + 2CO_{(g)} \quad (6)$$

Equation (6) is also an oversimplified view for the far more complex mechanism of ZrO_2 carbothermal reduction [4,5,18], which comprises of steps very similar to those of SiO_2 carbothermal reduction. Reaction (4) for the complete carbothermal reduction of zircon, thus, represents the sum of reactions (5) and (6).

An excess of carbon is preferred in order to suppress the loss of material by undesired reactions like the one presented by equation (7):

$$SiC + SiO_2 = 3SiO_{(g)} + CO_{(g)} \quad (7)$$

The excess of carbon should also prevent the occurrence of undesired reactions like the one presented by reaction (8), which can also lead to the loss of material during the CTR reaction of $ZrSiO_4$:

$$3SiC + 2ZrO_2 = 2ZrC + 3SiO_{(g)} + CO_{(g)} \quad (8)$$

Reaction (8) is possible because the formation of SiC precedes ZrC formation. According to the experimental observations and thermodynamic predictions based on free-energy calculations [5,18], formation of SiC is favoured at lower temperatures over the formation of ZrC, thus making SiC an effective reducing agent for ZrO_2 CTR reaction.

The aim of the this work was the development of improved, lower temperature processing routes for the production of ZrC/SiC, ZrO_2/SiC and ZrO_2 powders directly from raw materials with a minimum number of process steps.

II. Experimental

Commercially available zircon powder ($ZrSiO_4$, "Trebol", USA, ~ 40μm) was used as the starting material. Chemical analysis of the powder, given by the manufacturer, is as follows: ZrO_2 - 65%, SiO_2 - 33%, Al_2O_3 - 2%, TiO_2 - 0.35%, Fe_2O_3 - 0.05%. Activated carbon dried at 383 K (2 h) was used as a reducing agent ("Trayal", Serbia, ~ 10 μm, ashes ≤ 1%, specific surface area BET ~ 1000 m^2g^{-1}, AC in further text).

The $C/ZrSiO_4$ mixtures were prepared by mixing $ZrSiO_4$ with appropriate amounts of AC in order to obtain samples with the various molar ratios of carbon to zircon ($C/ZrSiO_4$ = 1, 4, 5 and 7). Carbothermal reduction of samples is performed in the 1573–1973 K temperature range (graphite crucibles, heating rate of 40 K/min, Ar flow atmosphere of 100 ml/min, 1 h soaking time) in a water-cooled vertical graphite furnace ("ASTRO", Santa Barbara, USA). Samples were cooled inside the furnace to the room temperature under Ar flow, removed from the furnace and decarburized at 873 K (2 h, air), in order to obtain ZrO_2 from ZrC and to remove any unreacted carbon.

Structural analysis (XRD) was carried out by a Siemens D-500 XRD powder diffractometer with CuK_α radiation (in conjunction with CuK_β nickel filter) on the products before and after decarburization process. The average crystallite size was calculated from well known Scherrer's formula:

$$\langle D \rangle = 0.9 \cdot \lambda / (\beta \cdot \cos\theta) \quad (9)$$

where $\langle D \rangle$ is the average crystallite size, λ is the wavelength of the X-rays, θ is the diffraction angle, β is corrected full width at the half maxima (FWHM).

Phase composition of samples is represented in a standard semi-quantitative way, by comparing intensities for the main (strongest) reflections of each phase (for example: $I_{ZrC}/I_{m\text{-}ZrO2} = x$; where $x = 0$ means that ZrC phase is absent, and $x = 100$ means that m-ZrO_2 phase is absent).

The microstructural study and energy dispersive analysis of X-rays (EDS) were performed on samples with Au/Pd coating with VEGA TS 5130 mm, TESCAN scanning electron microscope (SEM). Prior

to SEM/EDS analysis, samples were oxidized in air at 873 K (2 h), in order to remove the residual (unreacted) carbon which, if not removed, makes SEM/EDS analysis rather difficult.

III. Results and discussion

Phase content of $ZrSiO_4$ CTR reaction products in the temperature range of 1573–1973 K, can be seen in Table 1. SiC is identified in all samples as β-form (JCPDS number 29-1129). Other phases identified are: ZrC - JCPDS number 35-0784; m-ZrO_2 - JCPDS number 36-0420; c-ZrO_2 - JCPDS number 27-0997.

Influence of C/$ZrSiO_4$ ratio can be clearly observed from XRD patterns of samples heat treated at 1873 K (Fig. 1):

- monophasic material with all reflections belong to m-ZrO_2 was prepared when C/$ZrSiO_4$ = 1:1 (Fig. 1a),
- material with dominant ZrC phase and traces of m-ZrO_2 and c-ZrO_2 phases was prepared when C/$ZrSiO_4$ = 4:1 (Fig. 1b),
- material with dominant ZrC phase, traces of c-ZrO_2 and SiC phases and no trace of m-ZrO_2 phase was prepared when C/$ZrSiO_4$ = 5:1 (Fig. 1c) and
- material with dominant ZrC phase, considerable amount of SiC and traces of c-ZrO_2 phase, was prepared when C/$ZrSiO_4$ = 7:1 (Fig. 1d).

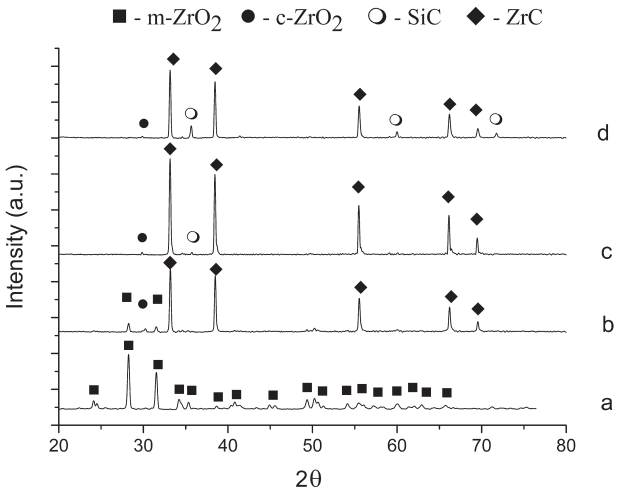

Figure 1. XRD patterns of samples with different C/$ZrSiO_4$ molar ratios heat treated at 1873K: a) 1:1, b) 4:1, c) 5:1 and d) 7:1.

Table 1. Phase composition and colour of the samples depending on temperature and C/$ZrSiO_4$ ratio

C:Zr ratio	1573 K	decarb.	1673 K	decarb.	1773 K	decarb.	1873 K	decarb.	1973 K	decarb.
C/$ZrSiO_4$ =1:1										
$ZrSiO_4$	100*	100	100	100	100	100				
m-ZrO_2	10	10	29	24	44	45	100	100	100	100
colour	black	light grey	dark grey	light grey	dark grey	light grey	dark grey	light gray	dark grey	cream
C/$ZrSiO_4$ =4:1										
$ZrSiO_4$	100	100								
m-ZrO_2	26	26	100	100	100	100	14	87	4	43
c-ZrO_2	7		5		4	10	5	100	t	100
SiC			21	20	23	20				
ZrC			4		54		100		100	
colour	black	light grey	dark grey	light gray	dark grey	light grey	black	light grey	black	cream
C/$ZrSiO_4$ =5:1										
$ZrSiO_4$	74	68								
m-ZrO_2	100	100	100	100	9	100				
c-ZrO_2	17		7	14	t	80	t	100	t	100
SiC			32	26	6	43	t	18	t	u
ZrC			71		100		100		100	
colour	black	light grey	black	light grey	black	light grey	black	light grey	black	light grey
C/$ZrSiO_4$ =7:1										
m-ZrO_2	100	100	21	100						
c-ZrO_2			5	90	6	81	t	100	t	100
SiC	26	27	29	96	15	100	18	84	22	87
ZrC			100		100		100		100	
colour	black	light grey	black	light gray	black	light grey	black	light grey	black	light gray

Legend: *decarb.* – after decarburization process (873 K, 2 h, air); *t* – traces; *u* – impossible to determine due to the overlapping;
* Intensity of the strongest peak

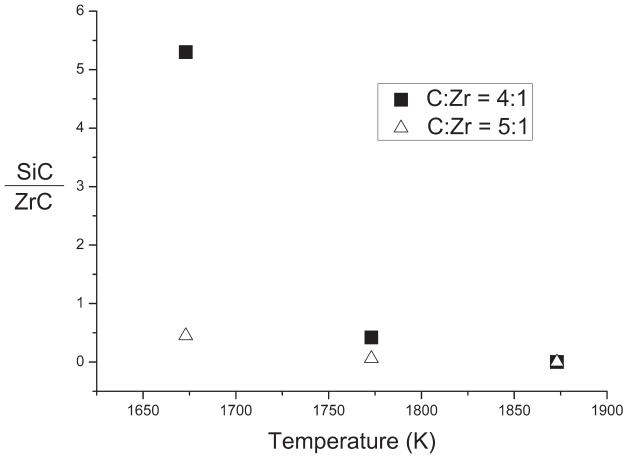

Figure 2. Change in SiC phase content for 4:1 and 5:1 samples in function of temperature

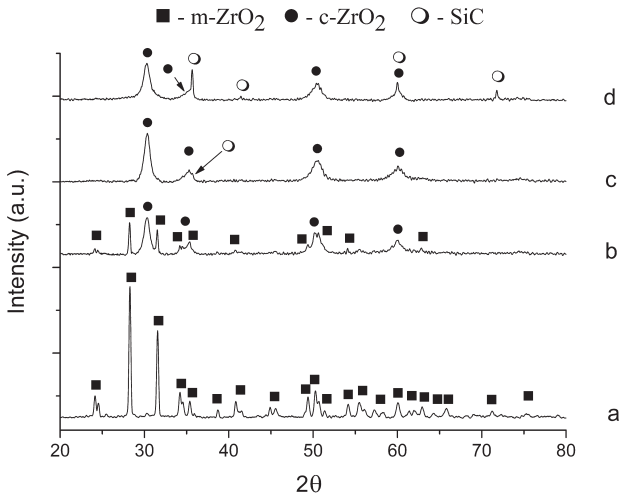

Figure 3. XRD patterns of samples heat treated at 1873 K after decarburization process: a) 1:1, b) 4:1, c) 5:1 and d) 7:1 C/ZrSiO$_4$ ratio

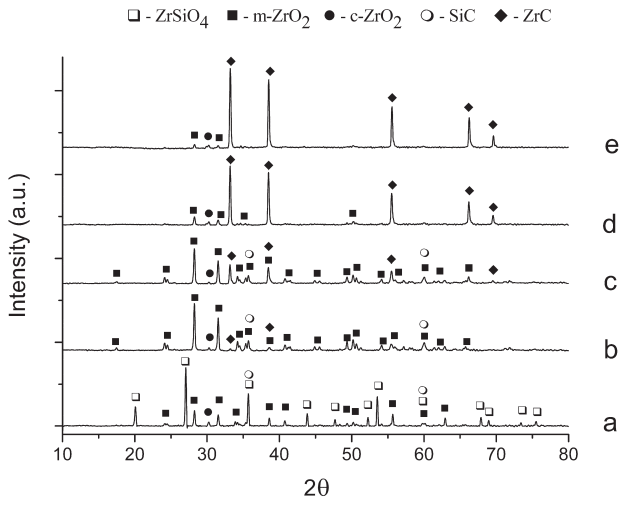

Figure 4. XRD patterns of sample with 4:1 C/ZrSiO$_4$ ratio, recorded at different temperatures: a) 1573K, b) 1673K, c) 1773K, d) 1873K and e) 1973K

As one can see from Fig. 1 and Table 1, the amount of ZrC formed increases with the increasing amount of carbon added. In sample with C/ZrSiO$_4$ = 5:1, the whole amount of m-ZrO$_2$ is consumed and transformed into the ZrC. It is also important to note that in this sample, a trace of SiC phase appears for the first time. The absence of the SiC reflections in the sample with C/ZrSiO$_4$ = 4:1 (Fig. 1b), means that the whole amount of SiC formed is used as reducing agent in ZrC synthesis, as represented by reaction (8). After the whole amount of m-ZrO$_2$ is transformed into the ZrC, remnants of the SiC phase appear in XRD spectrum (Fig. 1c). According to this, SiC content in samples with C/ZrSiO$_4$ = 7:1 (Fig. 1d) is much higher than in the samples with C/ZrSiO$_4$ = 5:1.

The change in phase content for the samples with 4:1 and 5:1 ratio is more conveniently presented in Fig. 2, by comparing the intensity ratios of strongest reflections for SiC and ZrC phase. In fact, Fig. 2 shows how the SiC content in these samples changes with temperature, and represents clear evidence that SiC is indeed consumed by reaction (8).

These observations are important because it is now absolutely clear that CTR reaction of ZrSiO$_4$ does not proceed as proposed by reaction (3). In the samples with C/ZrSiO$_4$ = 4:1 and 5:1, formation of SiC, represented by reaction (3) i.e. reaction (5), is only the first step of the reaction, followed immediately by reaction (8).

In the sample with 5:1 ratio, almost pure ZrC is obtained with only traces of SiC, which implies that pure ZrC can be obtained by varying carbon content around this point. Reactions (6) and (8) at 1873 K are obviously competitive in nature and that's why SiC content is higher in the samples with 7:1 ratio than in the sample with 5:1 ratio. If it would not be so, the SiC content would be the same as in the sample with 5:1 ratio. In other words, if more carbon is present – more SiC will "survive", because ZrO$_2$ will consume carbon that surrounds it, instead of SiC.

The XRD patterns of the samples heat treated at 1873 K and then decarburized in air (873K, 2h) are presented in Fig. 3. Phase composition of decarburized samples as observed from their XRD patterns is also given in Table 1. Thus, the prepared samples have: i) m-ZrO$_2$ phase when C/ZrSiO$_4$ = 1:1 (Fig. 3a), ii) m-ZrO$_2$ and c-ZrO$_2$ phase when C/ZrSiO$_4$ = 4:1 (Fig. 3b), iii) dominant c-ZrO$_2$ phase, traces of SiC and no trace of m-ZrO$_2$ phase, appears when C/ZrSiO$_4$ = 5:1 (Fig. 3c) and iv) dominant c-ZrO$_2$ phase and considerable amount of SiC phase when C/ZrSiO$_4$ = 7:1 (Fig. 3d). Obviously, oxidation at 873 K in air, transforms ZrC into the c-ZrO$_2$ in all samples. The m-ZrO$_2$ phase is present only in the samples where m-ZrO$_2$ was present before decarburization process. It can also be seen that reflections of c-ZrO$_2$ are much wider than those of preceding ZrC (≈ 0.2° for ZrC and ≈ 0.9° for c-ZrO$_2$) indicating that crystallites in

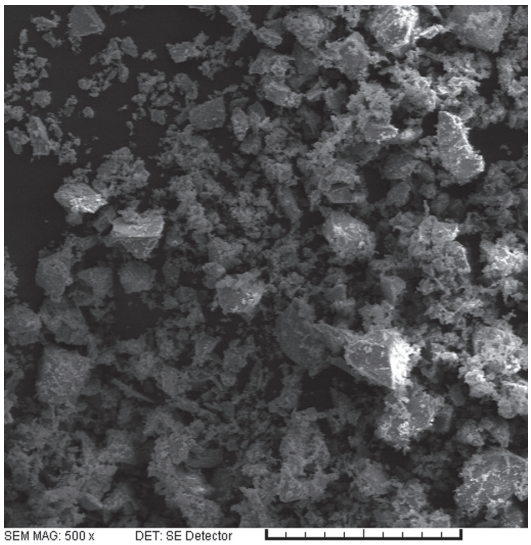

a)

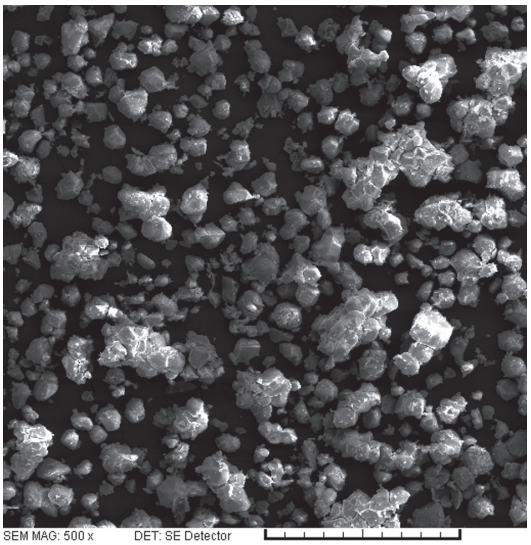

b)

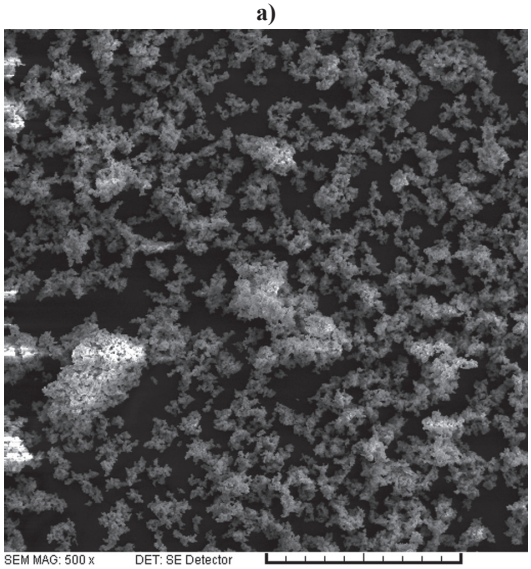

c)

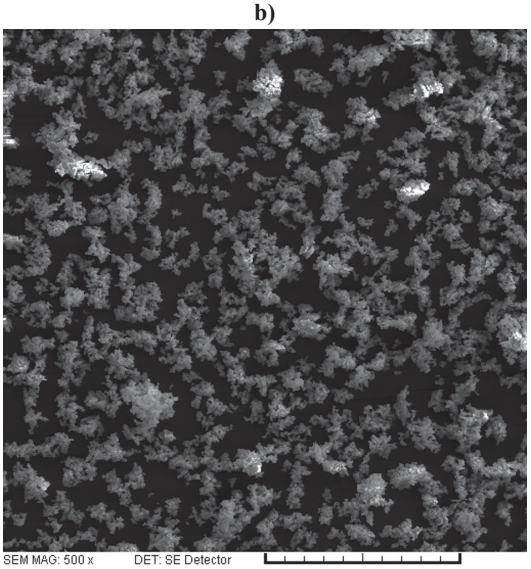

d)

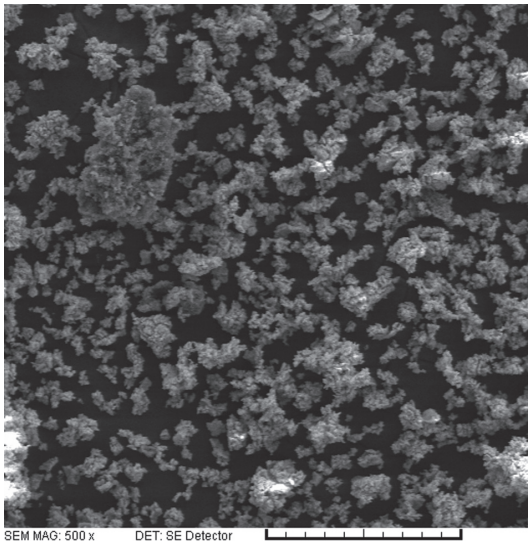

e)

Figure 5. SEM images of as-received $ZrSiO_4$ powder (a) and powders obtained after the heat treatement at 1873 K and decarburization process when $C/ZrSiO_4$ ratio was: b) 1:1, c) 4:1, d) 5:1 and e) 7:1

c-ZrO_2 are much smaller than those in ZrC (<*D*> ≈ 10 nm for c-ZrO_2, and <*D*> ≈ 40 nm for ZrC). Moreover, the calculated average crystallite sizes for c-ZrO_2 phase in our samples are in very good agreement with those observed by Shimada (2−10 nm) using HRTEM [9], for c-ZrO_2 samples obtained also by ZrC oxidation.

The change in phase composition of the samples after oxidation in air, presented in Table 1, is similar to that of samples before oxidation, simply because they are closely related to their predecessors: the only change is that ZrC is now completely converted into the c-ZrO_2 [9], while other phases are unaltered by oxidation process. For the sample with 5:1 ratio, SiC can now be clearly seen in XRD pattern of oxidized sample.

For the sample with 4:1 ratio at 1973 K decarburization process gives mixture of m-ZrO_2/c-ZrO_2. In the samples with 5:1 and 7:1 ratio at 1873–1973 K resulting products are a mixture of c-ZrO_2 and SiC. Also, low SiC content in the sample with 5:1 ratio at 1973 K indicates that it should be possible to obtain very pure c-ZrO_2 by slightly varying the carbon content and time/temperature of heat treatment.

As for the temperatures lower than 1873 K, Table 1 also gives us some useful information. There is no ZrC in any sample heat treated at 1573 K, only SiC phase is observed in the sample with 7:1 ratio. At this temperature $ZrSiO_4$ is dominant phase in the samples with 1:1 and 4:1 ratio, it is strongly present in the sample with 5:1 ratio and disappears only in the sample with highest carbon content (7:1). ZrC phase appears only after temperature is increased to 1673 K, and its content increases with increasing C/$ZrSiO_4$ ratio. At this temperature, $ZrSiO_4$ phase disappears in all samples except in that with 1:1 ratio. At 1773 K, ZrC content is generally higher than at 1673 K (as it can be observed from phase contents of 4:1 and 5:1 sample) and m-ZrO_2 content is lower than at 1673 K (5:1 and 7:1 sample). At 1873 K, m-ZrO_2 phase content further decreases in the samples with 4:1 and 5:1 ratio, followed by the simultaneous decrease in SiC content due to reaction (8), which is also responsible for the increase of ZrC content in these samples. Visually, these changes can most easily be seen in 4:1 sample, i.e. the change of its XRD patterns with temperature, as presented in Fig. 4.

Moreover, the colour of the samples is actually quite indicative of the phase composition of samples i.e. the progress of CTR reaction. These data is presented in Table 1, in which the phase composition and the colour of the samples are presented as a function of temperature and C/$ZrSiO_4$ ratio.

SiC phase is hard to observe in XRD patterns of samples at T≤1673 K, where SiC and $ZrSiO_4$ phase coexist together, because the main reflection of SiC overlapped

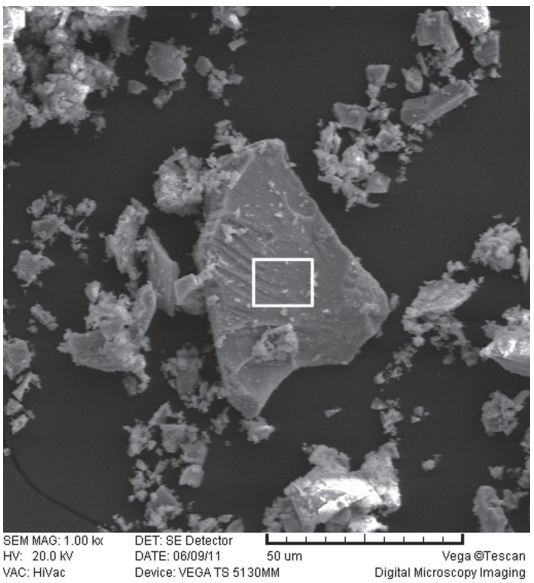

a)

Element	Wt.%	At.%
O	39.21	70.73
Si	13.95	14.44
Zr	46.17	14.72
Hf	0.67	0.11

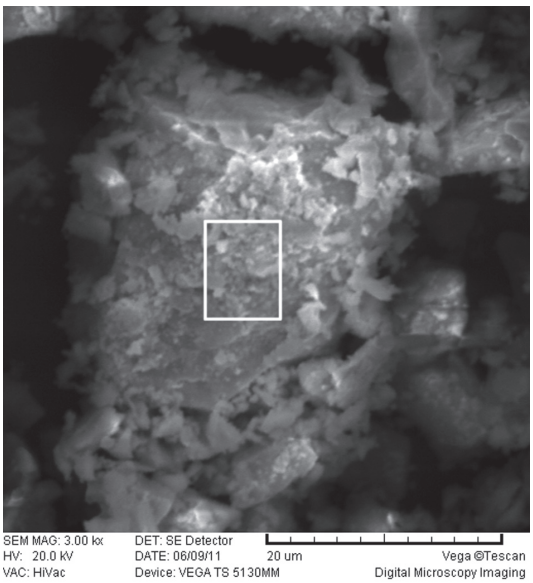

b)

Element	Wt.%	At.%
O	39.91	71.29
Si	13.55	13.74
Zr	45.81	14.32
Al	0.38	0.40
Ti	0.29	0.17
Fe	0.15	0.08

Figure 6. SEM/EDS analysis of $ZrSiO_4$ powder

with the strong reflection of $ZrSiO_4$ phase, thus making determination of SiC content very difficult. However, the light-grey colour of the samples after the decarburization process suggests that SiC phase is present in these samples. The formation of SiC at this temperature is observed in numerous studies considering the CTR process of SiO_2 and Mg-silicates [13,16,17,19–21]. At higher temperatures, main SiC reflection is usually quite distinguishable from weaker nearby reflections of m-ZrO_2 and c-ZrO_2. In the samples with higher SiC content, the presence of reflection at $2\theta \approx 72^o$ is also used as an evidence for undoubted presence of SiC.

The initial colour of all as-prepared C/$ZrSiO_4$ powder mixtures was black. As one can see, general rule is that decarburized samples are lighter in colour than their predecessors. The colour of the samples before decarburization is black or dark-grey. The colour of the decarburized samples is light-gray or creamy. The samples with 5:1 and 7:1 C/$ZrSiO_4$ ratio remain black after the CTR reaction at 1573–1973 K. This indicates the presence of free (excess) carbon in these samples.

By contrast, the change of colour from black to dark-grey in the 4:1 sample heated to 1673 and 1773 K, indicates that a part of the carbon is consumed in the CTR process at these temperatures. However, the most interesting observation is that at 1873 and 1973 K the colour of these samples turns black again. This can be explained by the increased content of ZrC in these samples at 1873 and 1973 K, because it is known that fine ZrC powders are black in colour. As already stated, the average crystallite size for ZrC in our samples is $\langle D \rangle \approx$ 40 nm, which indicates possible existence of very fine ZrC particles.

On the other hand, majority of the decarburized samples are light-grey in colour, with exception for the samples heat treated at 1973 K with 1:1 and 3:1 ratios (creamy colour). The creamy colour of the samples is indication that SiC phase is absent i.e. consumed by reaction (8).

The SEM micrographs and EDS spectra of the samples shown in Fig. 3 are presented in Figs. 5-10. Areas analyzed by means of EDS analysis are marked by white rectangles and the results are given in the tables beside the images.

The micrographs of the powders presented in Fig. 3, together with that of as-received $ZrSiO_4$ powder, are comparatively given in Fig. 5. As one can see, the appearance of heat treated powders is quite distinguishable from that of the starting $ZrSiO_4$ material. The starting $ZrSiO_4$ powder consists of particles that are irregular in both shape and size, but they are generally bigger than the particles of the heat treated powders. On the other hand, particles in 4:1, 5:1 and 7:1 sample, are quite similar by shape and size, and can be ea-

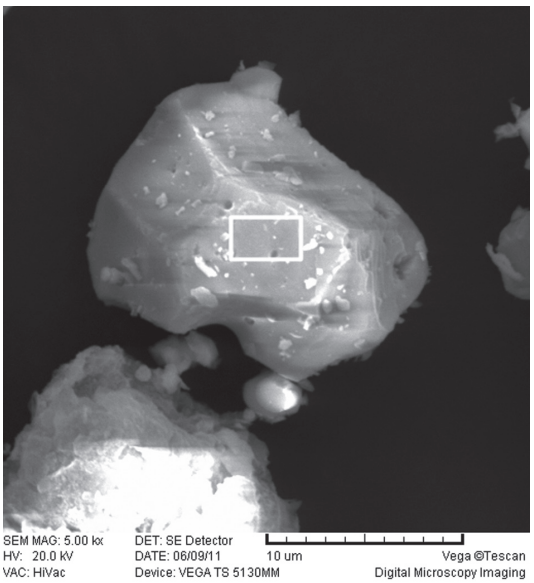

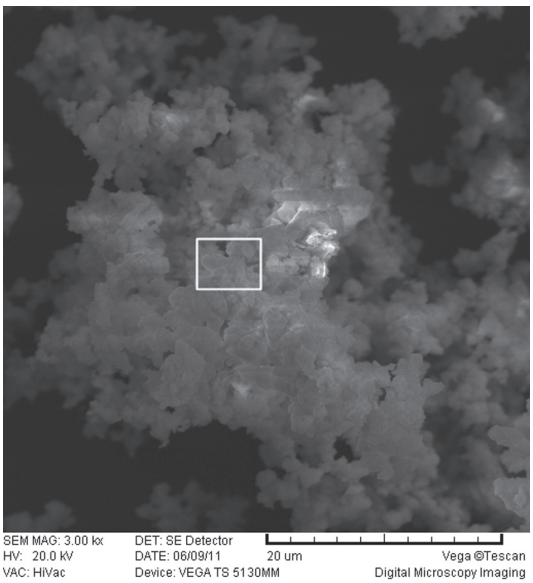

Element	Wt.%	At.%
O	28.67	69.61
Al	0.23	0.33
Zr	69.71	29.56
Hf	1.04	0.23
Ti	0.35	0.27

Figure 7. SEM/EDS analysis of sample with C/$ZrSiO_4$ ratio = 1:1

Element	Wt.%	At.%
O	29.29	69.16
Al	1.58	2.21
Zr	67.87	28.12
Hf	0.85	0.18
Ti	0.41	0.33

Figure 8. SEM/EDS analysis of sample with C/$ZrSiO_4$ ratio = 4:1

sily distinguished from those in $ZrSiO_4$ and 1:1 sample. 4:1, 5:1 and 7:1 powders consists of agglomerates of the very fine particles, while 1:1 powder consists of large polyhedral particles sintered together.

Detailed SEM/EDS analysis of as-received $ZrSiO_4$ powder is given in Fig. 6. EDS analysis of two big particles reveals that besides impurities declared by supplier (Fe, Ti and Al), as-received sample contains also Hf, which is invariably found [22] in zirconium ores (typically 0.5-3 wt.%).

The detailed SEM/EDS analysis of the sample with 1:1 C/$ZrSiO_4$ ratio is given in Fig. 7. The sample consists of large white polyhedral particles with size varying from ≈ 5 μm to ≈ 20 μm, as seen in Fig. 5b. The smooth and non-porous surface of one of these particles is shown in Fig. 7, together with results of the EDS analysis. As one can see, its chemical composition corresponds to that obtained by XRD analysis: ZrO_2 without a trace of Si-compounds (Fig. 3a).

The detailed SEM/EDS analysis of the sample with 4:1 C/$ZrSiO_4$ ratio is given in Fig. 8. Large white polyhedral particles are not observed in this sample, which instead consists of agglomerates of small particles, whose size does not exceed several μm. Chemical composition of one of these agglomerates, corresponds to that obtained by XRD analysis: ZrO_2 without a trace of Si-compounds (Fig. 3b).

The detailed SEM/EDS analysis of the sample with 5:1 C/$ZrSiO_4$ ratio is given in Fig. 9. Large white polyhedral particles are not observed in this sample, which instead consists of agglomerates comprising a small particles, whose size does not exceed several μm (Fig. 9). Chemical composition of one of these agglomerates (Fig. 9a), corresponds to that obtained by XRD analysis: ZrO_2 with a trace of Si-compounds (Fig. 3c) presumably SiC.

The detailed SEM/EDS analysis of the sample with 7:1 C/$ZrSiO_4$ ratio is given in Fig. 10. Large white polyhedral particles are not observed in this sample, which instead consists of agglomerates of small particles, whose size does not exceed several μm. However, two different phases can be clearly distinguished in this sample: porous phase consisting of smaller loose particles (Fig. 10b) and phase consisting of larger particles sintered together (Fig. 10a). Chemical composition of these agglomerates (Fig. 10a,b), corresponds to that obtained by XRD analysis (Fig. 3d): ZrO_2 phase (Fig. 10a) and SiC phase (Fig. 10b).

The ZrO_2 polyhedron forms are recognizable in the Fig. 10a, although the crystals tend to form clusters and it seems that many of the ZrO_2 crystals are sintered together. Although c-ZrO_2 phase consists of rather small crystallites (<*D*> ≈ 10nm), c-ZrO_2 particles are much larger (≥ 1 μm) then we expected on the basis of crys-

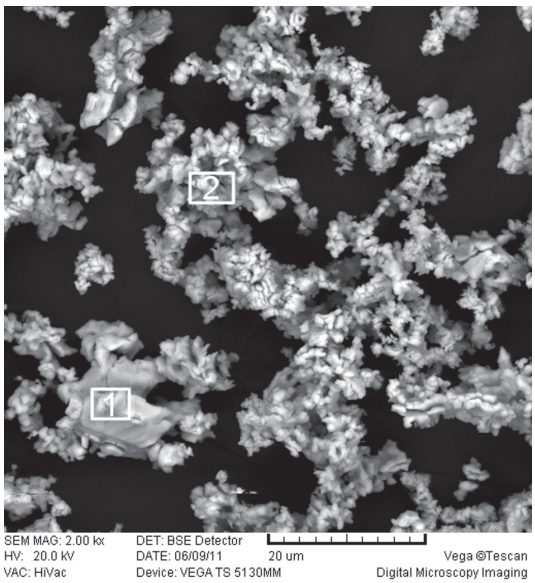

a)

Element	Wt.%	At.%
O	32.43	72.97
Al	0.30	0.39
Zr	65.41	25.77
Hf	0.86	0.18
Ti	0.38	0.29
Fe	0.62	0.40

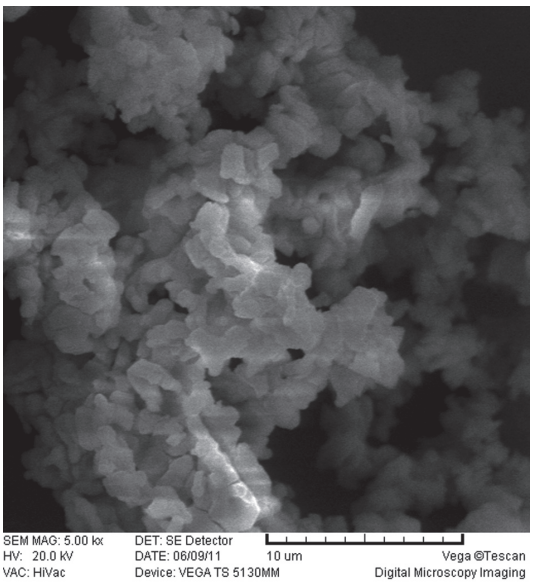

b)

Element	Wt.%	At.%
O	33.56	72.66
Al	0.13	0.17
Si	2.15	2.66
Zr	63.60	24.13
Fe	0.26	0.17
Ti	0.30	0.21

Figure 9. SEM/EDS analysis of sample with C/$ZrSiO_4$ ratio = 5:1

tallite size observed by XRD analysis. Also, the very low Si-content in the phase presented in Fig. 10a, confirmes that this is c-ZrO_2 phase comprising only a small amount of SiC.

The looser more porous phase, consisting of smaller particles irregular both in shape and size (Fig 10b), is SiC phase. The appearance is very similar to SiC phases observed in samples obtained by CTR reaction of natural Mg-silicates (sepiolite, asbestos, [19–21]). The very low oxygen content in this phase, also confirmes that this is SiC phase comprising only of a small amount of c-ZrO_2.

It can also be said, that according to EDS spectra, c-ZrO_2 and SiC phases in the 7:1 sample are obviously quite well separated and the powder consists of large aggregates.

Also, since these agglomerates seem to consist of particles sintered together, and that EDS analysis confirms the presence of impurities (Fe, Al, Ti, Hf) in them, it is quite possible that liquid phase/phases are formed on the grain boundaries. One of these phases, observed both in the literature and in our earlier studies, was iron-silicide. Iron-silicides have very low melting points, thus facilitating the transport of the material and manifesting themselves as catalysts in CTR reactions [20,21]. Formation of multiphase eutecticums is also possible due to the several impurities present in the as-received $ZrSiO_4$ (Fe, Al, Ti, Hf), but these liquid phases are difficult to prove by XRD and SEM/EDS analysis due to the limitation of instruments/methods. Only the TEM/EDS analysis could confirm their presence and location in the microstructure, but this is beyond our current capabilities.

IV. Conclusions

It has been shown that it is possible to obtain pure (or almost pure) m-ZrO_2 and c-ZrO_2 powders, as well as c-ZrO_2/SiC mixed composite powders after the heat treatment of zircon at relatively low temperatures. The process is relatively simple, consisting of two steps (carbothermal reduction/decarburization). It was shown that by altering the C/$ZrSiO_4$ ratio, various products could be obtained. Low carbon content (C/$ZrSiO_4$ ratio = 1:1) leads to the formation of m-ZrO_2, larger carbon content (C/$ZrSiO_4$ ratio = 5:1) favours the formation of almost pure c-ZrO_2 and the excess of carbon (C/$ZrSiO_4$ ratio = 7:1) drives the reactions towards the formation of c-ZrO_2/SiC mixed powders. According to the SEM/EDS analysis, c-ZrO_2 and SiC phase are obviously quite well separated and consist of large aggregated particles. It was also shown that although crystallite sizes (obtained by XRD anal-

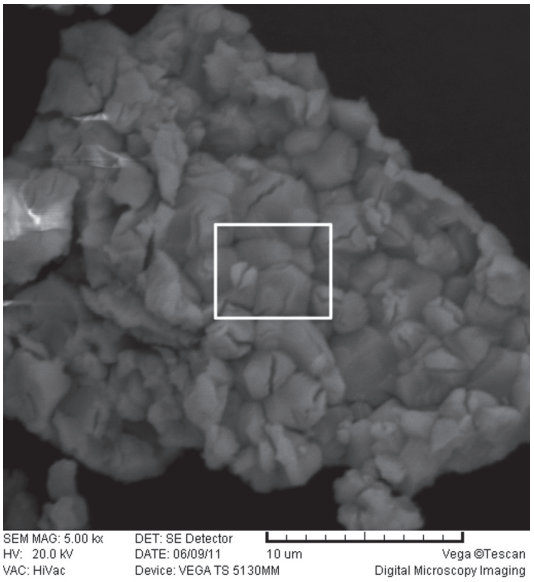

a)

Element	Wt.%	At.%
O	27.69	68.11
Al	0.31	0.43
Si	0.39	0.55
Zr	69.70	30.08
Hf	1.14	0.24
Ti	0.42	0.35
Fe	0.35	0.24

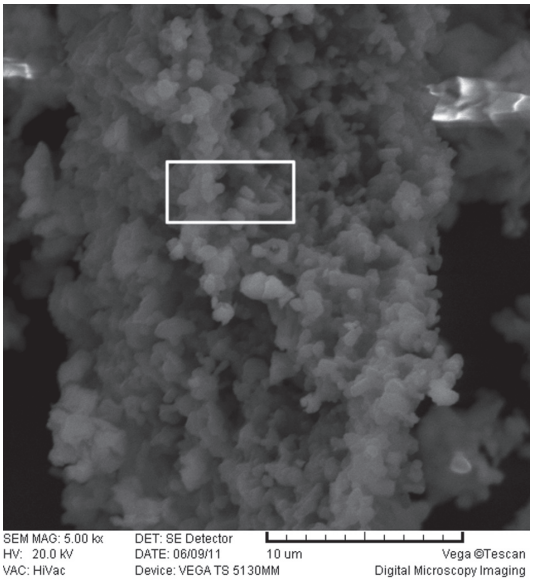

b)

Element	Wt.%	At.%
O	3.07	5.63
Al	1.97	2.14
Si	84.35	87.90
Zr	6.36	2.05
Ti	0.38	0.23
Fe	3.87	2.05

Figure 10. SEM/EDS analysis of sample with C/$ZrSiO_4$ ratio = 7:1

ysis) imply that c-ZrO_2 phase should be comprised of rather small or even nanoparticles, the SEM/EDS analysis of this phases shows that c-ZrO_2 particles are in fact much larger (≥ 1 μm) than expected.

Acknowledgments: This project was financially supported by the Ministry of Science and Environmental Protection of Serbia (project number: III-45012).

References

1. W. Honghzi, G. Lian, G. Jingkun, "Fabrication and microstructure of Al_2O_3-ZrO_2-SiC nanocomposites", *J. Eur. Ceram. Soc.*, **19** [12] (1999) 2125−2131.
2. L. Donzel, S.G. Roberts, "Microstructure and mechanical properties of cubic zirconia (8YSZ) SiC nanocomposites", *J. Eur. Ceram. Soc*., **20** [14-15] (2000) 2457−2462.
3. A.K. Soh, D.-N. Fang, Z.-X. Dong, "Analysis of Toughening Mechanisms of ZrO_2/nano-SiC Ceramic Composites", *J. Composite Mater*., **38** [3] (2004) 227−241.
4. B.-Y. Ma, J. Yu, "Phase composition of SiC-ZrO_2 composite materials synthesized from zircon doped with La_2O_3", *J. Rare Earths*, **27** [5] (2009) 806−810.
5. B.-Y. Ma, J.-K. Yu, Q. Zhu, Y. Sun, „Thermodynamic analysis and preparation of β-SiC/ZrO_2 composites", *Int. J. Miner. Metall. Mater.*, **16** [5] (2009) 581−585.
6. K. Komeya, *Fine Ceramics*, Ed. S. Saito, Elsevier Science Publ. Co., New York, 1988. p. 175.
7. M.H. Bocanegra-Bernal, S.D. de la Torre, "Phase transitions in zirconium dioxide and related materials for high performance engineering ceramics" (Review), *J. Mater. Sci.*, **37** [23] (2002) 4947−4971.
8. A. Kaiser, M. Lobert, R. Telle, "Thermal stability of zircon ($ZrSiO_4$)", *J. Eur. Ceram. Soc*., **28** [11] (2008) 2199−2211.
9. S. Shimada, "Microstructural observation of ZrO_2 scales formed by oxidation of ZrC single crystals with formation of carbon", *Solid State Ionics*, **101-103** [2] (1997) 749−753.
10. T.Y. Luo, T.X. Liang, C.S. Li, "Stabilization of cubic zirconia by carbon nanotubes", *Mater. Sci. Eng. A*, **366** [1] (2004) 206−209.
11. L. Combemale, Y. Leconte, X. Portier, N. Herlin-Boime, C. Reynaud, "Synthesis of nanosized zirconium carbide by laser pyrolysis route", *J. Alloys Compd.*, **483** [1-2] (2009) 468−472.
12. E. Djurado, P. Bouvier, G. Lucazeau, "Crystallite size effect on the tetragonal-monoclinic transition of undoped nanocrystalline zirconia studied by XRD and raman spectrometry", *J. Solid State Chem.*, **149** [2] (2000) 399−407.
13. D.H. Filsinger, D.B. Bourrie, "Silica to silicon: Key carbothermic reactions and kinetics", *J. Am. Ceram. Soc.*, **73** [6] (1990) 1726−1732.
14. V. Hlavacek, J.A. Puszynski, "Chemical engineering aspects of advanced ceramic materials", *Ind. Eng. Chem. Res.*, **35** [2] (1996) 349−377.
15. P.K. Panda, L. Mariappan, V.A. Jaleel, T.S. Kannan, A. Amroune, J. Dubois, G. Fantozzi, "Preparation of zirconia and silicon carbide whisker biphasic powder mixtures by carbothermal reduction of zircon powders", *J. Mater. Sci.*, **31** [16] (1996) 4277−4288.
16. G.C. Wei, "Beta SiC powders produced by carbothermic reduction of silica in a high-temperature rotary furnace", *J. Am. Ceram. Soc.*, **66** [7] (1983) C-111−C-113.
17. V.D. Krstić, "Production of Fine, High-Purity Beta Silicon Carbide Powders", *J. Am. Ceram. Soc.*, **75** [1] (1992) 170−174.
18. A. Maitre, P. Lefort, "Solid state reaction of zirconia with carbon", *Solid State Ionics*, **104** [1-2] (1997) 109−122.
19. A. Devečerski, A. Radosavljević-Mihajlović, A. Egelja, M. Pošarac, B. Matović, "Fabrication of SiC by carbothermal-reduction reactions of sepiolite", *Mater. Sci. Forum*, **555** (2007) 261−265.
20. A. Devečerski, M. Pošarac, A. Egelja, I. Pongrac, A. Radosavljević-Mihajlović, B. Matović, "SiC fabrication by carbothermal reduction of sepiolite", *J. Optoelectron. Adv. Mater.*, **10** [4] (2008) 876−879.
21. A. Devečerski, M. Pošarac, A. Egelja, A. Radosavljević-Mihajlović, S. Bošković, M. Logar, B. Matović, "Fabrication of SiC by carbothermal-reduction reactions of mountain leather asbestos", *J. Alloys Compd*., **464** [1-2] (2008) 270−276.
22. D.R. Lide, *Handbook of Chemistry and Physics*, CRC press, 84th edition, 2003-2004.